ZIBELINE INTERNATIONAL™ PUBLISHING

Earth Sciences Malaysia (ESMY)

DOI: http://doi.org/10.26480/esmy.02.2021.77.85

ISSN: 2521-5035 (Print)
ISSN: 2521-5043 (Online)
CODEN: ESMACU

RESEARCH ARTICLE

SOFT-SEDIMENT DEFORMATION STRUCTURES AND GRANULOMETRIC PROPERTIES DISTRIBUTION IN AJALI SANDSTONE RIDGES, WESTERN AFIKPO BASIN, UTURU, NIGERIA

Raphael Oaikhena Oyanyan*

Department of Geology, College of Environmental Sciences, Gregory University Uturu, P.M.B. 1012, Amaokwe Achara, Uturu, Abia State, Nigeria.
****Corresponding Author Email: raphoyanyan@yahoo.com***

ARTICLE DETAILS

Article History:

Received 05 August 2021
Accepted 07 September 2021
Available online 11 October 2021

ABSTRACT

Three Ajali sandstone ridges (L1, L2 and L3) at Uturu being quarried for construction sands were studied for soft-sediment deformation structures (SSDS) and granulometric properties distributions. SSDS that includes recumbents foresets, sands dykes, flame structures and fluid escape tubes were identified only in ridge L3. The geometry of the SSDS indicates sediment loading/density contrast, fluidization and liquefaction as the mechanisms for their formation but with liquefaction as the most dominant mechanism. Gran size analysis and granulometric curves properties calculations show that: Mean grain size ranged from fine (1.18 ϕ) to medium (2.57 ϕ); Sorting ranged from rarely poorly sorted (1.13ϕ) to well sorted (0.37ϕ) but with mean values in each ridge as moderate sorted; Skewness ranged from strongly fine skewed (1.0) to strongly coarse skewed (-1.57); and Kurtosis ranged from very platykurtic (0.27) to very leptokurtic (2.0) but with sands of ridge L3 mainly very platykurtic. Granulometric curves and bivariate plot of properties indicate fluvial deposition with rare marine influence. Results show that there is no significant variation in sediment properties and depositional environments across the three ridges. The localization of SSDS and non-proximity to any fault suggest that liquefaction, as the dominant mechanism for soft-sediment deformation, was not triggered by an earthquake. Possible mechanisms include rapid sediment loading, localised sudden subsidence induced by loading of localised oxidized compressible peats and coal; and increased in sediments' water saturation via localised groundwater seepage. Fine grains, well sorting, fine to strongly skewed very platykurtic characteristics of sediments made it more susceptible to liquefaction.

KEYWORDS

Ajali sandstone, Soft-sediment deformations, deformation mechanisms, grain sizes, granulometric properties, depositional environment.

1. INTRODUCTION

Soft-sediment deformation (SSD) occurs in sub-aqueously deposited sediment that retains some water after deposition (Nichols, 2009). It results in collapse of sediment framework in beds or changes to the fabric and layering of bed of recently deposited sediment preserved in ancient sedimentary rock as soft-sediment deformation structures (SSDS) (Nichols, 2009; Valente et al., 2014). They are attributed to sediment gravitational instabilities, loading; liquefaction and fluidization triggered by any factor that could be sediments density contrast, rapid sediment deposition, seismic shocks (or earthquakes), sudden subsidence, groundwater movement or seepages, movement of pressured pore fluids and sudden change in slope gradient (Knipe, 1986; Owen and Moretti, 2011; Pisarska-Jamrozy and Weckwerth, 2012).

Liquefaction, which is one of the most likely mechanism for SSD in subaqueous environment is when sediment particles loose contacts and become suspended in pore fluid (Boggs Jr., 2006). It occurs when grain weight is temporarily transferred to the pore fluid due to sudden shocks or series of shocks resulting in collapse of loosed packed grains fabric or increased in pore pressure (Boggs Jr., 2006; Owen and Moretti, 2011). Aftermath of shocks, whether seismic or non-seismic, can be uneven distribution of rate of subsidence in the basin. Sudden subsidence due to loading can also trigger non-seismic shocks which can in turn result in soft sediment deformation.

Apart from shocks, non-cohesive sediment particles can also be suspended in fluids and becomes fluidized when pressured fluids due to loading is released and injected to the base of the mass or column of the sediment and injection is continued until the grains are pushed apart (Boggs Jr., 2006). Sediment fluidization occurs when the upward drag exerted by moving pore fluid exceeds the effective weight of the grains (Selly, 2000). It makes the sediment to lose its strength or cohesiveness and behaves like a high viscous fluid that can flow rapidly. In fluidized sand beds, primary sedimentary structures are not usually preserved (Valente et al., 2014).

Apart from the aforementioned external factors that can trigger liquefaction and fluidization of sediment, there are also other properties of unconsolidated sediment that makes it susceptible to plastic or soft sediment deformation. They include grain size, clay content, bed thickness, packing density or porosity and degree of saturation (Owen and Moretti, 2011). Except the grain sizes, soft sediment deformation can result in change in other properties and in general on hydraulic properties

Quick Response Code	Access this article online	
	Website: www.earthsciencesmalaysia.com	**DOI:** 10.26480/esmy.02.2021.77.85

Cite The Article: Raphael Oaikhena Oyanyan (2021). Soft-Sediment Deformation Structures and Granulometric Properties Distribution in Ajali Sandstone Ridges, Western Afikpo Basin, Uturu, Nigeria.*Earth Sciences Malaysia, 5(2): 77-85.*

of sediment. Sands' clay content can decrease through vertical upward movement of fluidized clay matrix. Repacking of sediment grains following SSD results in decrease in bed thickness, porosity and permeability as well as change in hydraulic flow direction. Whereas grain sizes, which reflects weathering and erosion processes which generate particles of various sizes and the nature of subsequent transport processes, are well preserved in ancient deposits (Boggs Jr., 2006). Also, the duration of liquefied state under which soft sediment plastic deformation occurs is a function of the grain size (Owen and Moretti, 2011). And coarse silt to fine sands are more susceptible to liquefaction (Crespellani et al., 1988; Moretti et al., 1999; Owen and Moretti, 2011). Therefore, the study of granulometric properties (grain sizes distribution) can contribute in determining the factors that triggers the formation of SSDS preserved in ancient sedimentary rocks.

SSDS were identified in one of the three Ajali sandstone ridges of Afikpo basin at Uturu being quarried for civil construction sands. Two ridges where no SSDS was identified have been studied for lithofacies distribution, architectural elements and environment of deposition by Oyanyan et al. (2021). They interpreted the ridges based on the lithofacies characteristics and architectural elements as consisting of sandy braided fluvial successions underlain by marine successions. The third ridge with SSDS unequivocally shows the same lithofacies and architectural elements. The question then is, why should evidences of SSD be identified only in one out of the three ridges of sandstone in the same geographic wing of a basin?

Based on the foregoing, the main aim of this study was to find out why SSDS were found only in one ridge out of the three studied ridges. Therefore, the objectives of the study and the publication of this paper include 1) the documentation of the SSDS identified and the granulometric properties distribution in the studied Ajali sandstone ridges, 2) to find out if difference in mean grain sizes and other properties of granulometric curves, as preserved properties, could have aided the soft sediment plastic deformation in one location, 3) the determination of the mechanisms for the SSD and 4), the validation of the environment of deposition using grain size trend and bivariate plot of granulometric properties since textural characteristics of sediments are related to provenance, sedimentary processes, and sedimentary dynamics (Oyanyan et al., 2019). It is hoped that the granulometric properties described here can be used as a guide in the use of gravel packing for sand control in the development of sandy braided reservoir successions in oil and gas production (Calson et al., 1992).

1.1 Study Area and Geologic Setting

The area of study is located at the western end of Afikpo basin, a sub-basin in the southern Benue trough of Nigeria (Figure1). The Benue Trough is about 800km long failed rift basin that runs diagonally from Northeast to Southwest of Nigeria (Benkhelil, et al.1998; Ofoegbu, 1990). It is connected to the western and Central rift system of Africa (Fitton, 1980). The formation of Benue trough dates back to the late Jurassic/early Cretaceous when as a result of convection current in the asthenosphere, the Gondwana super-continent rifted at a triple rift direction junction, resulting in separation of the South American plates from the Africa plate via two of the three rifting directions (Nwajide, 2005). But opening in the third rifting direction failed to open up for the successful emplacement of oceanic plate, but formed a fault bounded long basin as an aulacogen called the Benue trough. The Trough had contiguous stable platforms. The southern part called the Abakaliki trough had the Anambra platform in the west and Ikpe platform in the east (Burke et al., 1972; Whiteman, 1982). In the Santonian, there was collisional thermotectonic event and reverse of the early Jurassic/ early Aptian tectonic episode. The thermotectonic event resulted in the compression and subsequent upliftment of the Abakaliki trough to form the Okigwe-Abakaliki anticlinorium; and the down-warp or flexural inversion of the Anambra and Ikpe platform to form the Anambra and the Afikpo basins respectively (Burke et al., 1972; Whiteman, 1982; Guiraud, 1983).
Basins in the southern Benue Trough had subsidence that was spasmodic or in phases of different rate. It was high in pre-Albian, low in Cenomanian and high in Turonian (Nwajide, 2005). The subsidence of Albian – Turonian was in response to cooling and contraction of the lithosphere that was thermally agitated by mantle upwelling or convection current in the asthenosphere during the rifting phase, while the post Turonian subsidence was mainly due to sediment loading (Nwajide, 2005; Ekine and Onuoha, 2008).

1.2 Stratigraphic Setting

Eustacy and tectonic subsidence created accommodation space for sediment deposition and preservation in southern Benue Trough. The sediment deposition has been attributed to three cycles of marine transgression and regression (Amajor, 1987; Benkhelil, et al.,1998; Akande et al., 2011). The first and second cycles resulted in the deposition of the pre- Santonian sediments which includes Asu River group (Aptian – Albian) and Eze-Aku / Agwu / Keana Formations (Late Cenomanian – Turonian). The third cycle resulted in the deposition of the Campanian-Maastrichtian sediments in Afikpo and Anambra basins. The Campano-Maastrichtian sediments called proto-Niger deltaic sequences comprised the basal marine Enugu/Nkporo Formation and the Coal Measures (deltaic Mamu Formation, Fluvial or fluviomarine Ajali and Nsukka Formations). The Campanian Nkporo Formation consist predominantly of shale and local occurrences of limestone and sandstone, while the overlying Mamu Formation consists of sandstone, shale, mudstone, siltstone and coal seams (Amajor, 1978; Onyekuru and Iwuagwu, 2010). The Maastrichtian Ajali Formation next in the sequence consist predominantly of sandstone, while overlying Nsukka Formation have similar characteristics as the Mamu Formation.

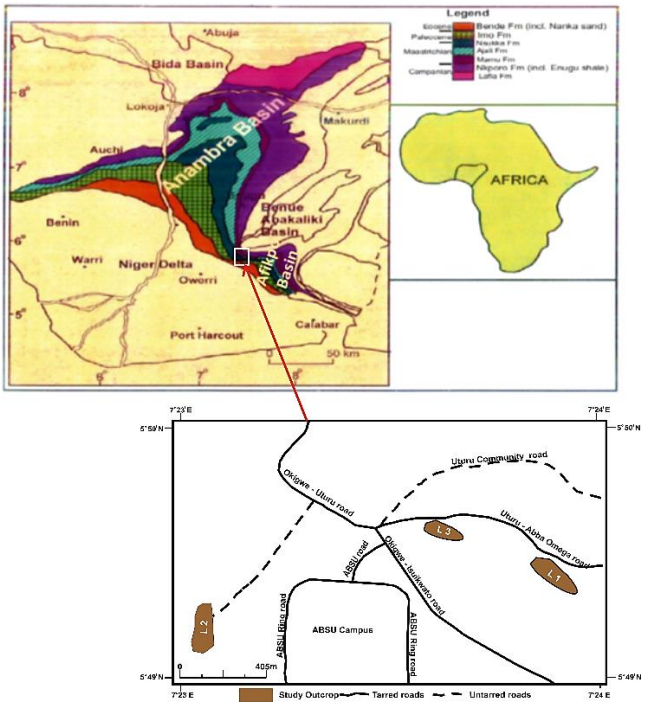

Figure 1: Geological map of Anambra and Afikpo basins of southern Benue Trough (Modified after Uzoegbu and Ikwuagwu, 2016). The insert shows the study outcrops locations and the access roads (Modified after Oyanyan et al., 2021).

1.3 Documented Characteristics of Ajali sandstone

The Ajali sandstone outcropped at Uturu, Nigeria, off axis of the Abakaliki anticlinorium, has been studied by some authors at different outcrop locations within Afikpo and Anambra basins (Figure 1). It was described as false bedded sandstone by Simpson (1954) and named Ajali sandstone by Reyment (1965). Amajor (1987), based on the analysis of paleocurrent and petrographic data classified it as quartz arenite with multi-cycled origin and mainly sourced from Abakaliki Anticlinorium. But Uzoegbu and Ikwuagwu (2016), through petrographic analysis of samples classified it as sub-feldspathic arenite. Adekoya et al. (2011) described it as shallow marine (littoral) deposit based on lithofacies characteristics, while Onyekuru et al. (2017), using bivariate plots of calculated granulometric parameters differentiated Ajali sandstone as river or fluvial deposit in agreement in with Hoque and Ezepue (1977) who had also attributed it to fluvial deposition. Ladipo (1985) classified Ajali sandstone in a location in Anambra basin as shallow marine sub-tidal sand bars.

2. Data Set and Methods of Study

The study began with visits to the three ridges where sedimentary structures and lithology types are well exposed as a result of processes of sandstone quarry for civil construction sands. The ridges were labelled ridge location (L) 1, 2 and 3 accordingly. The ridge L1, L2 and L3 have coordinates of 5° 49.629'N/7° 24.276'E, 5° 49.4281'N/7° 23.239'E and 5° 49.705'N/7° 24.061'E respectively. Ridge L3 is about 400m from L1 and 1.4km from L2 (Figure 1b). The vertical quarry faces of the ridges were surveyed for SSDS. The methodology of analyzing soft sediment

deformation structures proposed by Owen and Moretti (2011) was partly adopted. It includes identification of soft sediment deformation mechanism, recognition of soft sediment deformation structures due to liquefaction triggered by seismic and non-seismic shocks; and analyzing the geometry of the identified SSDS. Closed-up pictures of structures were taken with a digital camera. A measuring tape was used to measure the width of structures where necessary.

For the granulometric analysis of samples, the steep vertical quarry face permitted samples collection at every 1.5m from the bottom of ridge up to 3.5m. For each ridge location, bottom, middle and top samples were appropriately labelled A, B and C respectively. At ridge location 3, bottom sample was taken where there was no evidence of soft sediment deformation, whereas the middle and the top samples were taken from the deformed zone. The granulometric analysis was initiated by measuring between 250 to 450g of an ovum dried sample with an electronic weighing balance. The sample was then screened through sets of millimetre sized sieves strapped tight on an electronic shaker. It was shaken for 15 minutes based on the methods of Folks and Warden (1957) and Folks (1980). The sieve sizes were later converted to phi (ϕ) scale using the equation 1 below by Krumbein (1934).

$$\phi = -\log_2(d) \qquad d = \text{grain diameter (mm)} \qquad (1)$$

The weight of sample retained in each sieve was weigh and its percentage of the initial measured sample calculated as percentage weight retained. The calculation of cumulative weight of sample retained and plotting of cumulative percentage weight distribution and histogram of percentage weight of sample retained against grain sizes in phi (ϕ) units on arithmetic graph paper were done with Microsoft excel software. Phi values at 5%, 25%, 16%, 50%, 75%, 84% and 95% were determined from the cumulative frequency curves. The values were then inputted into Folks and Warden (1957)'s formulas for the determination of properties of the granulometric curves which include mean grain sizes, inclusive graphic standard deviation (sorting), inclusive graphic skewness and kurtosis. Grain size classification was done using Udden–Wentworth scale (Wenthworth, 1992) and grain-size triangle of Folks (1980). Phi values at 50% of the cumulative frequencies correspond to the median grain sizes. The steepest points (points of inflection) on the cumulative frequency curves and the highest points on the histograms were used to infer the modal grain size of each sample. Vertical grain size trend in each samples location was used to infer depositional systems and validated by bivariate plot of grain size sorting or standard deviation against skewness after Friedman (1967).

3. Results and Interpretations

3.1 Soft Sediment Deformation Structures (SSDS).

This section presents the different types of SSDS that were only identified in ridge L3 (Figure 2). They are as follows:

3.1.1 Recumbent foresets structures

Recumbent foresets appears as convolute bedding on the side view with asymmetric anticlines (Figure 3). The nose of the anticlines points in the downstream direction of south east, while the axis is parallel to the base of the deformed unit. About 70% of the sands in the ridge L3 is affected by this type of deformation. It is a plastic deformed cross stratifications similar to that described as fully developed folding (sheath folding) by Pisarska-Jamrozy and Weckwerth (2012). It is attributed to vertical passage of water through loosely packed sand or the deformation of liquefied sand by shear stress as it avalanches the lee slope of subaqueous sand dune (Selly, 2000; Nichols, 2009). The deposits can be described as recumbent folds formed by the deformation of liquefied sediment by current drag following a shock (Allen and Banks, 2006). It resulted in grains falling into a tighter packing. They are found in diverse traction-deposited sands, and are especially common in coarse sands of braided alluvium (Selly, 2000).

3.1.2 Clastic dykes

Sand dykes that pierced through recumbent forests or folds (Figure 4). It pinches at foreset boundary and swell within the foresets. The thickness decreases upward from average of 6 to 1cm. The vertical lengths of the dykes ranged from 1 to 4m. The upward decrease in thickness differentiated it from fissure fill which is an evidences of cracks by earthquake (Boggs jr. 2006; Nichols, 2009). Piercing through the deformed cross beds indicates formation after the plastic deformation of the cross beds. It is an evidence of fluidized quicksand or the product of elutriation of sand as a result of fluidization of large body of subsurface sediment (Selly, 2000; Nichols, 2009). It occurs when fluid pressure exceeds both tensile strength of the horizontal bed boundaries seals and the principal horizontal stress (Knipe, 1986; Ortner, 2007). It therefore suggests that this dykes were formed when fracture occurs above an over-pressured bed and the upward rush of sediment laden pore waters carries sediment into the crack (Nichols, 2009).

Figure 2: Distant view of ridge (L3), showing soft sediment deformation structures (recumbent foresets, sand dykes and flame structures). The height of the man in the Figure is 1.72m.

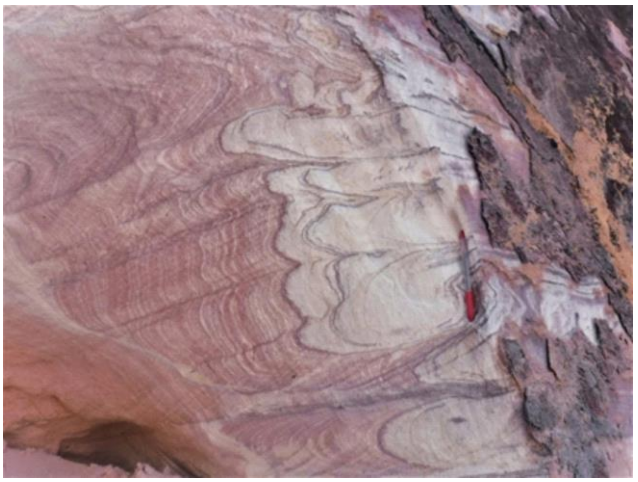

Figure 3: Recumbent forests in accreted sand bars with ferruginized accretion surfaces.

Figure 4: Sand dykes pierced through sets of recumbent foresets.

3.1.3. Fluid escape tubes

Localized highly liquefied and fluidized ferruginous cemented sedimentary units, characterized by fluid escape tubes of different orientations (Figure 5). The tubes are less than 3cm in diameter. It was identified at the base of deformed sequences of recumbent foresets. It shows complete destruction of primary beddings which suggest local fluidization due to fluid pressure greater than the grain weight (Knipe, 1986; Ortner, 2007). The complex fluidization may have been exacerbated by biogenic burrows.

Figure 5: Localized complex network of fluid escape structures (tubes) in highly liquefied and fluidized ferruginous cemented deposit grading upward to recumbent foresets.

3.1.4. Flame structures

Tongue of mud pushed into vertically oriented laminated sands in localized locations at the base of the column of sands affected by soft sediment deformation (Figure 6). It is formed by loading less dense water-saturated mud layers with denser sand and consequently the less dense materials squeezed upward into the overlying sand layers (Boggs Jr., 2006). The vertical oriented laminations indicate that the flame structure was formed before the deformation of overlying sands into recumbent folds or vertical laminations due to liquefaction. It also suggests rapid sediment loading as one of the possible triggers for the liquefaction.

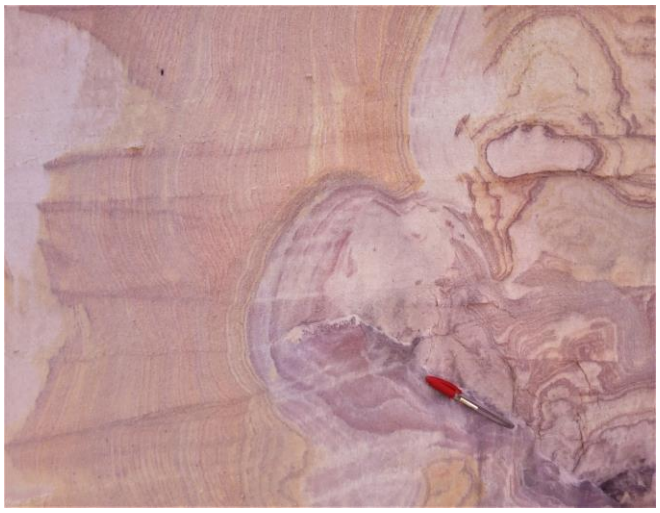

Figure 6: Flame structure in vertically oriented laminated sands.

3.2 Granulometric Properties

This section presents the results of particles size analysis of samples from the three Ajali sandstone ridge locations. The granulometric or ogive curves and histograms of the grain sizes are presented as Figures 7, 8 and 9. The specified percentile values from the curves for the determination of granulometric properties are presented in Table 1. The derived granulometric properties which includes mean grain sizes, inclusive graphic standard deviation (sorting), inclusive graphic skewness and kurtosis are presented in Table 2 and interpreted as follows:

3.2.1 Grain sizes

Grain sizes is a function of the materials available and the energy imparted on the sediments (Folks, 1980). Therefore, the vertical trend of changes in grain sizes can be used to infer the change in energy condition during the processes of sediment deposition and subsequent prediction of the type of depositional system. The granulometric curves (Figures 7A, 8A and 9B) show vertical fining upward successions with grain sizes decreasing from granules or coarse sand at the bottom to fine sand at the top reflecting decreasing strength or energy in a typical fluvial depositional system. However, the derived inclusive graphic mean grain size in ridge L1 and 2 is medium sand, while that of the L3 characterized by SSDS is fine sand (Table 2). But data approximation indicates quite similarity in grain sizes for L1 and L3 samples. The range of mean grain size from fine to medium is in line with the findings of Uzoegbu and Ikwuagwu (2016). The histogram of all the samples shows modal grain sizes changing from medium sands (1.23ϕ or 1.74ϕ) in L1 and 2 bottom samples to fine sand (2.74ϕ) in middle and top samples (Figures 7 and 8), while in L3 the modal grain size is fine sand (2.74ϕ) from bottom to the top. However, the histograms show unimodal distribution for all samples from all the locations indicating single source which is the nearby Okigwe-Abakaliki anticlinorium (Amajor 1987).

3.2.2 Inclusive graphic standard deviation (sorting)

Inclusive standard deviation gives the sorting of sediment. It is a measure of variation in grain sizes in a unit of sediment or sedimentary rock. It is a function of the material supplied to the environment, the type of deposition and the current characteristics or competency and efficiency of transporting agent (Folks 1980; PettiJohn, 1975). Irrespective of the materials supplied to the environment and type of deposition, a constant current, whether low or high will give better sorting than fluctuating current (Folks 1980). Therefore, it can be used to infer the maturity and distance of travel of sediment as well as the energy of the environment of deposition. The granulometric curves (Figures 7A, 8A and 9B) shows increase in sorting from bottom samples to the top samples reflecting an increased in the steadiness or stability of current though decreasing in strength or energy. The calculated inclusive graphic standard deviation values (Table 2) show that sorting of L1 and L2 bottom samples ranged from moderated sorted and poorly sorted respectively to moderately well sorted top samples and both with mean inclusive graphic standard deviation value indicating moderately well sorted sediment. The sorting for L3 samples grade from poorly sorted (1.13ϕ) bottom samples to well sorted (0.37ϕ) top sample but with mean inclusive graphic standard deviation similar to others. It shows that L3 samples are better sorted in middle and top samples as a result of more competent and efficient current though sandstone in the study area is generally moderately sorted indicating similar depositional environment and same source.

3.2.3 Inclusive graphic skewness

Skewness is the degree of asymmetry of sediment grain size population or the lopsidedness of the distribution curve or the degree of deviation from normal Gaussian curve that is symmetrical (Selly, 2000; Boggs Jr. 2006). It shows the sorting in the tails of sediment grain size population. Skewness can either be positive (fines) or negative (coarse). Excess of fines at the tail is said to be fine skewed or positively skewed, while excess of coarse particles at the tail is said to be coarse skewed or negatively skewed (Boggs Jr. 2006). The histograms of all the samples reflects skewness in the sediment grain size population (Figures 7A, 8A and 9B). Similarly, mode, median and mean values of grain sizes being of different values indicate skewness (Table 2). The calculated inclusive graphic skewness values give the quantitative measure of skewness of each sample (Table 2). L1 samples, from bottom to top are strongly positive skewed indicating fluvial environments consisting traction load (coarse grain) with infiltrating fine grains or suspended load (Folks, 1980). But for the L2 and L3, the bottom and middle samples of the former and bottom sample of the latter are strongly negative skewed, indicating large proportion of coarse materials, while their top samples are strongly positive skewed to positive skewed. The gradation from strongly negative skewness from the bottom to positive skewness at the top can be attributed to typical internal grading in accretionary macroform sedimentary architectural element of braiding fluvial system in L 2 (Oyanyan et al., 2021).

3.2.4 Kurtosis

Kurtosis is a measure of the peakness or sharpness in grain-size frequency curve (Folks, 1980; Boggs Jr. 2016). It compares the sorting of the sediment grains at the centre of the curve to that of the tail. It is a normal Gaussian distribution with kurtosis equals to 1.0 if the sorting in the tails equals to the sorting in the central portion. Where the centre is more sorted, it is leptokurtic and where it is more sorted at the tail, it is platykurtic. It also shows the dominance of part of the grain-size frequency curve. Leptokurtic indicates the dominance of the centre over the tail, while platykurtic indicates both the centre and tail are sub-equals. Therefore, kurtosis is a quantitative measure of departure from normality (Folks, 1980). The calculated kurtosis values of L1 and 2 samples varied and ranged from 0.45 (very platykurtic) to 2.0 (very leptokurtic) while that of L3, characterised by SSDS, are all very platykurtic (Table 2). It shows slight different paleo-condition of sediment deposition in ridge L3.

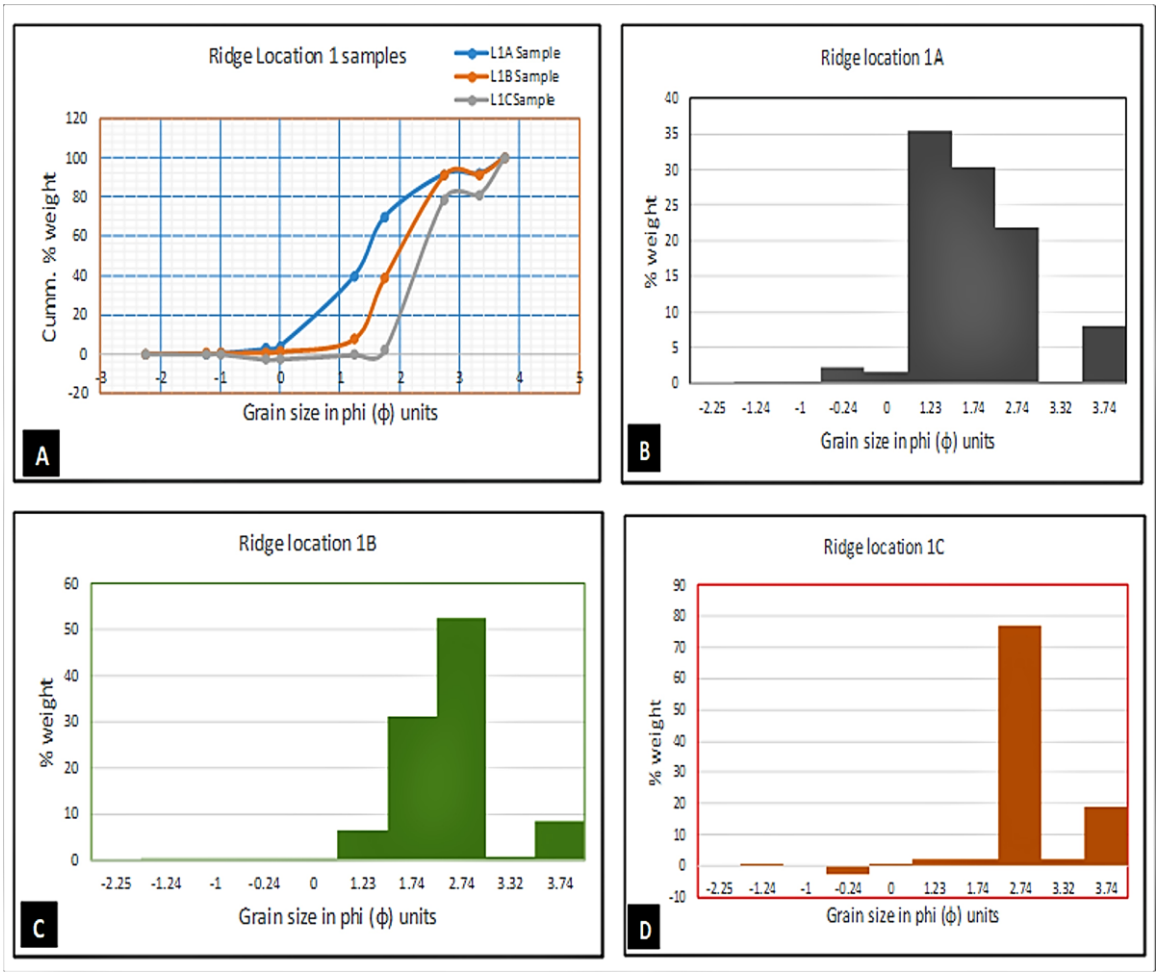

Figure 7: (A) The granulometric curves, (B, C andD) Histograms of bottom (1A), middle (1B) and top (1C) samples from ridge location 1 (L1). The granulometric curves shows grain size trend while the histograms show changes in modal grain sizes.

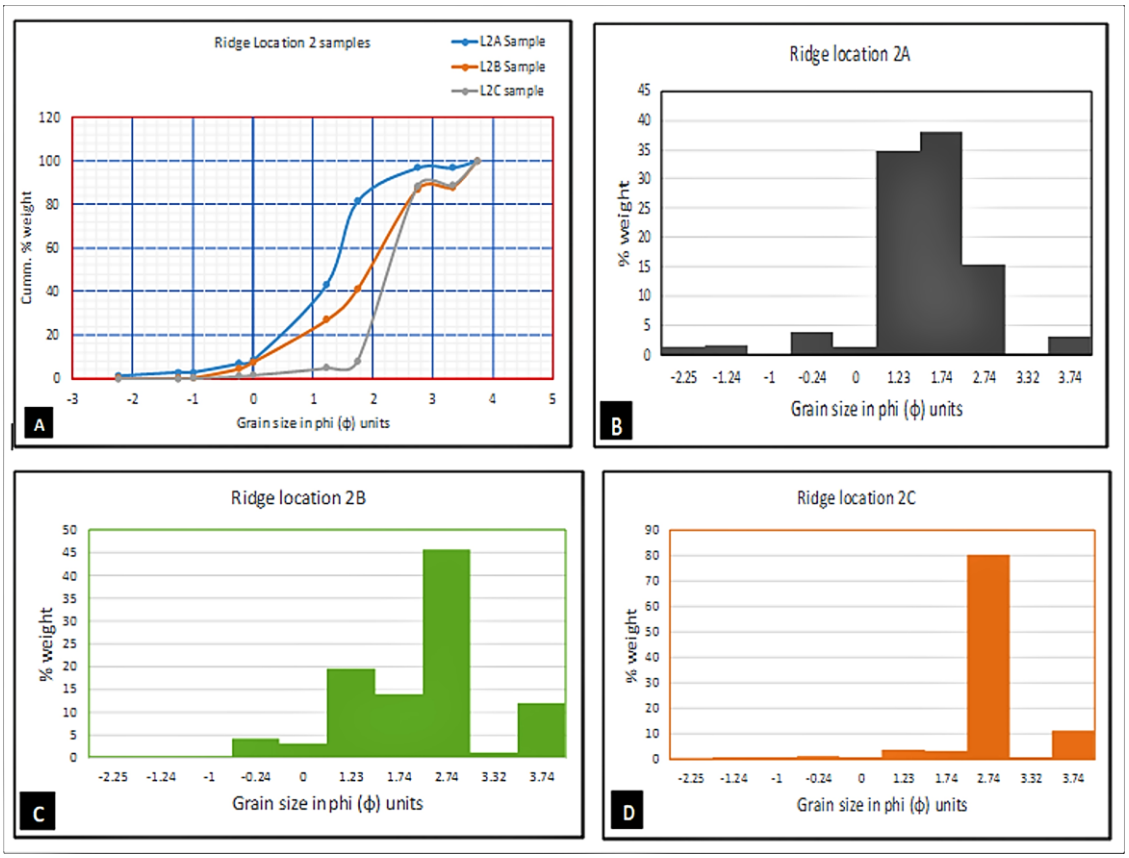

Figure 8: (A) The granulometric curves, (B, C and D) Histograms of bottom (2A), middle (2B) and top (2C) samples from ridge location 2 (L2). The granulometric curves shows grain size trend and sorting while the histograms show changes in modal grain sizes.

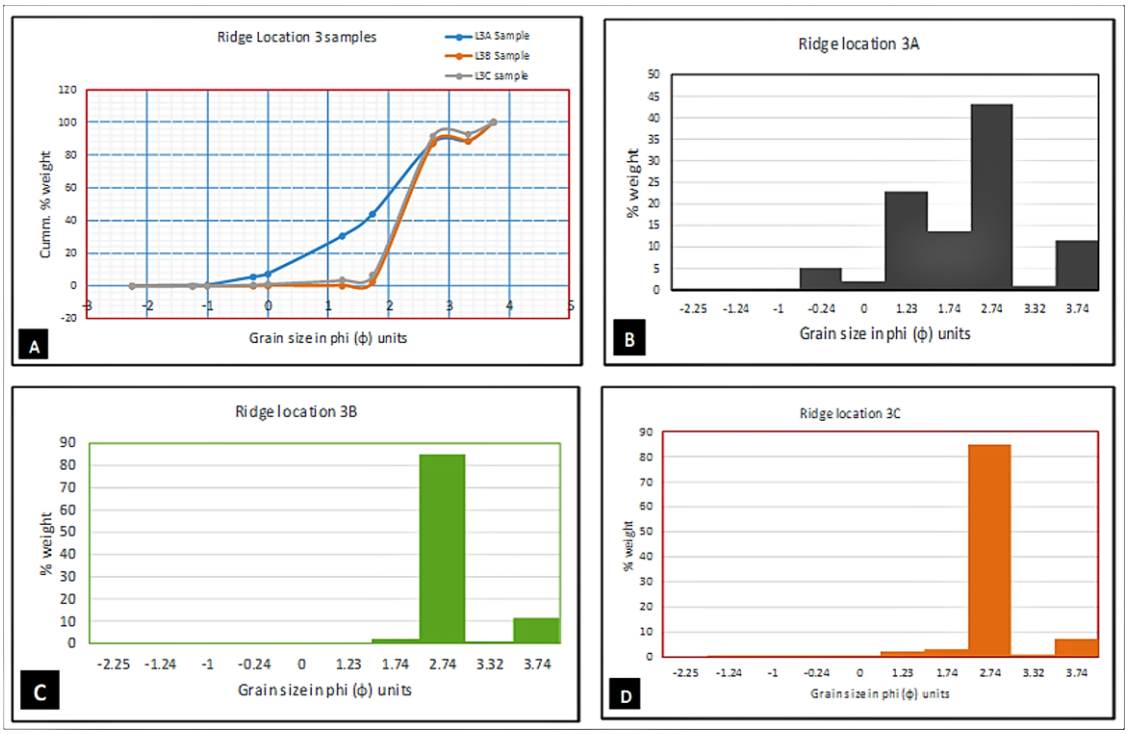

Figure 9: (A) The granulometric curves, (B, C and D) Histograms of bottom (3A), middle (3B) and top (3C) of samples from ridge location 3 (L3). The granulometric curves shows grain size trend and sorting while the histograms show same modal grain sizes.

Table 1: Measures from Granulometric Curves for Statistical Calculations

%	L1A ϕ sizes	L1B ϕ sizes	L1C ϕ sizes	L2A ϕ sizes	L2B ϕ sizes	L2C ϕ sizes	L3A ϕ sizes	L3B ϕ sizes	L3C ϕ sizes
95	3.5	3.55	3.65	2.58	3.6	3.55	3.6	3.6	2.9
84	2.3	2.6	3.42	1.8	2.65	2.65	2.62	2.7	2.62
75	1.93	2.32	2.65	1.6	2.38	2.55	2.4	2.58	2.52
50	1.42	1.97	2.35	1.38	1.9	2.22	1.85	2.3	2.2
25	0.75	1.50	2.05	0.6	1.1	1.98	0.98	2.02	1.98
16	0.45	1.45	1.95	0.35	0.6	1.85	0.5	1.98	1.85
5	-0.1	1.05	1.8	- 0.7	- 0.2	1.2	- 0.38	1.8	1.7

Table 2: Statistical parameters of grain sizes

Samples/ Parameters	L1A	L1B	L1C	L2A	L2B	L2C	L3A	L3B	L3C
Median grain size (ϕ)	1.42 M S	1.97 M S	2.35 F S	1.38 M S	1.9 M S	2.22 F S	1.85 M S	2.3 F S	2.2 F S
Mean median size (ϕ) per location	1.91 Medium sand			1.83 Medium sand			2.11 Fine sand		
Graphic mean grain size (ϕ)	1.39 M S	2.01 F S	2.57 F S	1.18 M S	1.72 M S	2.24 F S	1.65 M S	2.32 F S	2.22 F S
Mean graphic mean grain size per location (ϕ)	1.99 Medium/fine sand			1.71 Medium sand			2.06 Fine sand		
Inclusive GSD (sorting) (ϕ)	1.0	0.68	0.66	0.87	1.1	0.56	1.13	0.45	0.37
Mean inclusive GSD (sorting) per location (ϕ)	0.78 Moderately sorted			0.84 Moderately sorted			0.65 Moderately well sorted		
Inclusive graphic Skewness	0.9 SPS	0.86 SPS	1.0 SPS	-1.0 SNS	-1.3 SNS	0.72 SPS	-1.57 SNS	0.75 SPS	0.15 PS
Kurtosis	1.74 VLK	0.84 PK	0.45 VPK	1.34 LK	2.0 VLK	0.54 VPK	0.62 VPK	0.41 VPK	0.27 VPK

Acronyms: GSD = Graphic standard deviation, SPS = Strongly positive skewed, SNS = Strongly negative skewed, PS = Positive skewed, VLK = Very Leptokurtic, LK = Leptokurtic, VPK = Very platykurtic, PK = Platykurtic, M S = Medium sand, F S = fine sand.

3.2.5 Bivariate plots

The bivariate plot of skewness versus sorting of grain sizes can indicate the environment field of sediment deposition (Friedman, 1967). The bivariate plots of the calculated inclusive graphic skewness versus inclusive graphic standard deviation (sorting) of the nine samples from the three Ajali sandstone ridge locations show that all samples fell within the fluvial environment field except one top sample from ridge location 3 (Figure 10). It shows dominance of fluvial deposition but also suggest marine influence in the late stage of deposition in the Ajali sandstone ridge L3, characterized by SSDS. This finding of Ajali sandstone at Uturu being mainly deposited in fluvial environment field is also in agreement with the findings of Tijani et al. (2010); Uzoegbu and Ikwuagwu (2016); Oyanyan et al. (2021).

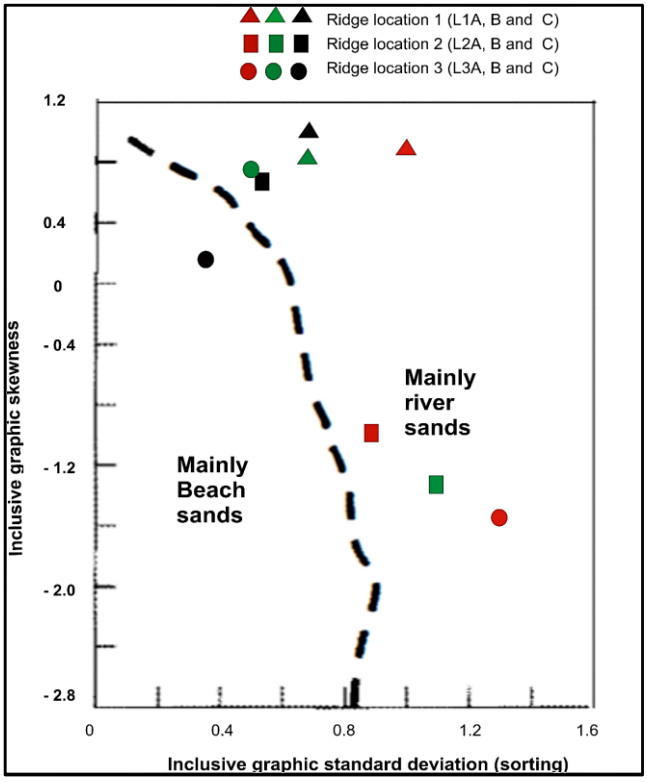

Figure 10: Bivariate plot of inclusive graphic skewness versus inclusive graphic standard deviation (sorting) (after Friedman, 1967).

4. DISCUSSIONS

4.1 Sediment Properties and Depositional Environment Across the Three Outcrops

The granulometric analysis of sediment samples from the three Ajali sandstone outcrops have revealed sediment properties and paleo-environment of deposition of sediment in the different outcrops. Each outcrop samples shows fining upward units from medium to fine grains, typical of channel or fluvial depositional environment (Selly, 2000; Nichols, 2009). Most of the samples from the studied outcrops are moderately to well sorted indicating high porosity and permeability (Table 2).

Though grain size trends are quite similar in all the outcrops, the granulometric curves properties (mean, sorting, skewness and kurtosis) distributions show slight differences in the classifications of the samples (Table 3). Mean grain size of all L1 and L2 samples are medium grains while that of L3, characterized by SSDS is fine grains (Table 3). All bottom samples have mean grain size as medium sand but varied in sorting, ranging from poor to moderate, skewness either strongly coarse or strongly fine and, kurtosis ranging from very leptokurtic to platykurtic. These slight variations across outcrops is consistent with the findings of Tijani et al. (2010); Uzoegbu and Ikwuagwu (2016). However, most of the middle (excluding L2) and top samples are classified as fine sand, moderately to well sorted, fine to strongly fine skewed very platykurtic. It indicates no significant variation in the upper sequences in the ridges. The slight differences in the sediment properties of the bottom or channel floor sediments samples can be attributed to the dynamisms in energy condition of fluvial depositional system attributed to dynamic climatic conditions and slope gradient.

Table 3: Summary of sediment classification across the three outcrops.

Location	Samples	Classifications
L1	C (Top)	Fine sand, moderately well sorted, strongly fine skewed very platykurtic
	B (Middle)	Fine sand, moderately well sorted, strongly fine skewed platykurtic
	A (Bottom)	Medium sand, moderately sorted, strongly fine skewed very leptokurtic
L2	C (Top)	Fine sand, moderately well sorted, strongly fine skewed very platykurtic
	B (Middle)	Medium sand, poorly sorted, strongly coarse skewed very leptokurtic
	A (Bottom)	Medium sand, moderately well sorted, strongly coarse skewed leptokurtic
L3	C (Top)	Fine sand, well sorted, fine skewed very platykurtic
	B (Middle)	Fine sand, well sorted, strongly fine skewed very platykurtic
	A (Bottom)	Medium sand, poorly sorted, strongly coarse skewed very platykurtic

4.2 The Soft Sediment Deformation Mechanisms and Their Triggers

The geometry of the identified SSDS in ridge L3 revealed the most plausible possible mechanisms for their formations. Recumbent foresets and fluid-escape structures (sand dykes and tubes) indicate liquefaction and fluidization respectively, while flame structures indicate rapid sediment loading/density contrast. The preservation of stratifications in most parts of the stratigraphic unit, the association of deformed bed with fluid escaped structures and the absence of brittle features strongly suggest liquefaction as the main mechanism for the SSD (see Owen and Moretti, 2011). The triggers for the liquefaction of sediment can either be seismic (earthquake) or non-seismic factors (Obermeier, 1996; Owen and Moretti, 2011). For sediment to be susceptible to liquefaction it must be characterized by fine- to medium-grains, high water saturation, permeability barriers, low overburden pressure or shallow burial and high porosity (see Crespellani et al., 1988; Obermeier, 1996; Moretti et al., 1999; Owen and Moretti, 2011). The lithofacies analysis of the studied outcrops by Oyanyan et al. (2021) and the granulometric analysis in this study show that the three Ajali sandstone ridges have similar distribution of gran sizes, lenticular mudstones as permeability barriers, highly porous cross bedded units and subaqueous depositional environments in the upper sequences that could have made all the ridges to be characterized by SSDS.

The main allogenic trigger of liquefaction is earthquake. An earthquake with a moment magnitude of 5–6 can generate liquefaction and fluidization features up to 10 km from the epicentre (Obermeier, 1996). Consequently, SSDS attributed to liquefaction triggered by earthquakes should be proximal to faults, pervasive, and correlative across different outcrops, except where there are some significant variations in sediment properties such as grain sizes, mud content, bed thickness and degree of water saturation (see Owen and Moretti, 2011). Apart from grain size kurtosis, slight difference in sorting in middle and top samples (Tables 2 and 3), the three studied outcrops have similar distribution of primary sediment properties with no significant variations that can halt the pervasiveness of earthquake induced shocks required for sediments' liquefaction. Therefore, earthquake is ruled out as the trigger for the liquefaction that resulted in the formation of SSDS in ridge L3. Furthermore, non-seismic and autogenic factors are considered as triggers for the liquefaction of the sediment. The possible non-seismic triggers for the mechanisms of the SSD in L3 are rapid sediment supply, rapid compaction or compression of underlying formation, sudden subsidence induced by loading of compressive underlying formation and increased in sediments' water saturation via localised groundwater seepage.

Apart from faults and crustal thermal anomaly controlled subsidence that characterised especially the early evolution phase of the lower Benue Trough, sediment loading contributed more to the subsidence in the later phase (Ekine and Onuoha, 2008). The rate of sediment load induced subsidence across the basin could not have been uniform but varied due to varied thicknesses and characteristics of the sediment load. Mamu Formation that directly underlays the Ajali Formation consists of compressive peat/coal seams with thicknesses and compressibility that

vary across the basin (Oladapo et al., 2008). Therefore, in ridge L3, quick sediment loading of localised oxidized compressible peats and coal of Mamu Formation could have resulted in localised sudden subsidence with associated shocks that triggered localised liquefaction and fluidization (see Gambolati et al., 2003; Van Asselen, 20011). However, the fine grains, well sorting, fine to strongly skewed very platykurtic characteristics of the ridge L3 sediments made it more susceptible to liquefaction possibly triggered by the sudden subsidence (Table 3). It also shows that apart from regional subsidence and eustacy, local subsidence also contributed to the creation of accommodation space for sediment deposition and preservation in the western end of Afikpo basin where Ajali sands were deposited.

5. Conclusions

The following conclusions can be drawn from this study:

1. Mean grain size range from fine to medium. Grain size sorting ranged from rarely poorly sorted to dominantly moderate – well sorted. Skewness ranged from strongly fine skewed to strongly coarse skewed grains but with strongly fine skewed grains most dominant. Kurtosis ranged from very platykurtic to very leptokurtic but with sands of the ridge with soft sediment deposition structures mainly very platykurtic.

2. Granulometric curves of rock samples and bivariate plot of its properties from each Ajali sandstone ridge indicate mainly river deposition with very rare marine influence.

3. The grain size histograms show unimodal distribution for all samples from the three Ajali sandstone ridges indicating single source.

4. Soft-sediment deformation structures (SSDS) formed by liquefaction, fluidization and quick sediment loading/density contrast were only identified in ridge location (L) 3. They include recumbents foresets, sands dykes, flame structures and fluid escape tubes. Since there is no significant variation in sediment properties across the three ridges; and there is non-pervasiveness and non-correlation of SSDS across the three outcrops as well as non-proximity of location to any fault, therefore earthquake as triggering mechanisms for the deformation is ruled out.

5. The possible mechanisms for the soft-sediment deformation (SSD) include rapid sediment supply/loading, rapid compaction or compression of underlying formation, localised sudden subsidence induced by loading of localised oxidized compressible peats and coal of Mamu Formation and increased in sediments' water saturation via localised groundwater seepage.

6. The fine grains, well sorting, fine to strongly skewed very platykurtic characteristics of the ridge L3 sediments made it more susceptible to liquefaction that triggered the SSD.

7. Apart from regional subsidence and eustacy, local subsidence also contributed to the creation of accommodation space for sediment deposition and preservation in Afikpo basin.

Acknowledgement

The Author is sincerely grateful to the Department of Geology, Gregory University, Uturu, Nigeria and the management of the University for the facilities used for this research..

References

Adekoya, J.A., Aluko, A.F., Opeloye, S.A., 2011. Sedimentological characteristics of Ajali sandstone in the Auchi environs of Anambra basin, Nigeria. Ife Journal of Science, 13(2), Pp. 52-67.

Akande, S. O., Egenhoff, S. O., Obaje, N. J., Erdtmann, B. D., 2011. Stratigraphic Evolution and Petroleum Potential of Middle Cretaceous Sediments in the Lower and Middle Benue Trough, Nigeria: Insights from New Source Rock Facies Evaluation. Petroleum Technology Development Journal: An International Journal, 1, Pp. 1 – 34. ISSN 1595-9104

Amajor, L.C., 1987. Paleocurrent, petrography and provenance analyses of the Ajali Sandstone (Upper Cretaceous), southeastern Benue Trough, Nigeria. Sedimentary Geology, 54, Pp. 47–60.

Allen, J. R.L., Banks N., 2006. An interpretation and analysis of Recumbent-folded deformed cross-beddings. Sedimentology, 19, 3-4, Pp. 257-283.

Benkhelil, J., Mascle, J., Guiraud, M., 1998. Sedimentary and Structural Characteristics of the Cretaceous Along the Côte D'ivoire-Ghana Transform Margin and In The Benue Trough: A Comparison. In Mascle, J., Lohmann, G.P., Moullade, M. (Eds.), Proceedings of Ocean Drilling Program, Science Results, 159, Pp. 93 -99.

Burke, K.C., Dessauvagie, Y. F. J., Whiteman, A. J., 1972. Geological history of the Benue valley and adjacent areas. In. T.F.J. Dessauvagie and A. J. Whiteman (Ed), African Geology University of Ibadan press, Ibadan, Pp. 187 – 205.

Boggs Jr., S., 2006. Principles of Sedimentology and Stratigraphy. Fourth Edition. Pearson Prentice Hall, USA, Pp. 676.

Carlson, J., Gurley, D., King, G., Price-Smith, C., Waters, F., 1992. Sand Control: Why and how? Oilfield Review, Schlumberger Oilfield Services publication, Pp. 41 – 53.

Crespellani, T., Nardi, R., Simoncini, C., 1988. La liquefazione del terreno in condizioni sismiche. Zanichelli, Bologna, Pp. 185.

Ekine, A. S., Onuoha, K.M., 2008. Burial history analysis and subsidence in Anambra basin, Nigeria. Nigerian Journal of Physics, 20, 1, Pp. 145-154.

Gambolati, G., Putti, M., Teatini, P., Storri, G.G., 2003. Subsidence due to peat oxidation and its impact on drainage infrastructures in a farmland catchment, South of the Venice Lagoon. RMZ-Materials and Geoenvironment, 50, 1, Pp. 125-128.

Guiraud, M., 1993. Late Jurassic-Early Cretaceous rifting and Late Cretaceous transpressional inversion in the Upper Benue basin (NE Nigeria). Bulletin-Centres de Recherches Exploration —Production Elf-Aquitaine Memoire, 17, Pp. 371–383.

Folk, R.L, Ward, W.C.1957. Brazos river bar: A study in the significance of grain-size parameters. Journal of Sedimentary Petrology, Pp. 27, 3–26.

Folks, R. L., 1980. Petrology of Sedimentary rocks. Hemphill Publishing Company, Austin, Texas 78703, USA. Pp. 190.

Friedman, G. M., 1 967, Dynamic processes and statistical parameters compared for size frequency distribution of beach and river sands: Journal of Sedimentary Petrology, 37, Pp. 327-354.

Hoque, M., Ezepue, C. M., 1977. Petrology and Paleogeography of Ajali Sandstone. Jounal of Nigerian Mining and Geosciences Society. 14, Pp. 16 – 22.

Knipe, R.J., 1986. Deformation mechanism path diagrams for sediments undergoing lithification. Memoir of Geological Society of America, 166, Pp. 151–160.

Krumbein, W. C., 1934, Size frequency distribution of sediments: Journal of Sedimentary Petrology, 4, Pp. 65-77.

Ladipo, K.O., 1985. Tidal shelf depositional model for the Ajali sandstone, Anambra basin, southern Nigeria. Journal of Africa Earth Sciences, 5, Pp. 172-185.

Nichols, G. 2009. Sedimentology and Stratigraphy. 2nd Edition. A John Wiley and Sons, Ltd., Publication, Pp. 432.

Obermeier, S.F., 1996. Use of liquefaction-induced features for paleoseismic analysis. Engineering Geology 44, Pp. 1–76.

Ofoegbu, C. O., 1990 (ed.). The Benue Trough: Structure and Evolution. Friedr Vieweg and Sohn, Braunschweig, Weisbaden, Pp. 359.

Oladapo, M.I., Adeoye-Oladapo, O.O., Alao, T.O., 2008. Geoelectric Study of Coal Deposits at Unwana/Afikpo Area of Southeastern Nigeria. Journal of Applied Sciences Research, 4, 11, Pp. 1534-1545.

Onyekuru, S. O., Iwuagwu, C. J., 2010. Depositional Environments and Sequence Stratigraphic Interpretation of the Campano-Maastrichtian Nkporo Shale Group and Mamu Formation Exposures at Leru-Okigwe Axis, Anambra Basin, Southeastern Nigeria. Australian Journal of Basic and Applied Sciences, 4(12), Pp. 6623-6640.

Onyekuru, S.O. Okoro, Eze M., Opara, K.D., Agumanu, A.E., Ikoro, D.O., 2017. Paleoenvironment and Provenance Studies of Ajali Sandstone in Igbere Area, Afikpo Basin, Nigeria. The International Journal of Engineering and Science (IJES), 6, 2, Pp. 19-30.

Ortner, H., 2007. Styles of soft-sediment deformation on top of a growing fold system in the Gosau Group at Muttekopf, Northern Calcareous Alps, Austria: Slumping versus tectonic deformation / Sedimentary Geology, elservier publication, 196, Pp. 99–118.

Oyanyan, R. O., Nwachukwu, Ohaegbulem, M. C., Iloanya, N. S., 2019. Sedimentological and Geochemical Characterization of Surficial Sediment of a Meander Section of Mbaa River at Nneise–Ugiri Community in Imo State of Nigeria. Journal of Geography, Environment and Earth Science International (JGEESI), 22, 1, Pp. 1-13. Article no. JGEESI.48882. ISSN: 2454-7352

Oyanyan, R.O., Ohaegbulem, M. C., Agbo, C. C., Iloanya, N. S., 2021. Sedimentary Architectural Elements and Sandy Braided Fluvial Successions in Ajali Sandstone Ridges, Western Afikpo Basin, Uturu, Nigeria. Earth Sciences Malaysia, 5, 1, Pp. 49-57.
DOI: http://doi.org/10.26480/esmy.01.2021.49.57

Owen, G., Moretti, M., 2011. Identifying triggers for liquefaction-induced soft-sediment deformation in sands. Sedimentary Geology, 235, Pp. 141–147

Moretti, M., Alfaro, P., Caselles, O., Canas, J.A., 1999. Modelling seismites with a digital shaking table. Tectonophysics, 304, Pp. 369–383.

Nwajide, C. S., 2005. Anambra Basin of Nigeria: Synoptic Basin Analysis as a Basis for Evaluating its Hydrocarbon Prospectivity, In Okogbue C. O. (eds). Hydrocarbon Potentials of the Anambra Basin: Geology, Geochemistry and Geohistory Perspectives. Proceedings Of the First Seminar Organised by Petroleum Technology Development Fund (PTDF) chair in Geology, University of Nigeria, Nsukka, Pp. 1 – 46.

Pettijohn, F. J., 1975. Sedimentary Rocks, 3rd edn.: Harper and Row, New York, NY., Pp. 718.

Pisarska-Jamrozy, M., Weckwerth, P., 2012. Soft-sediment deformation structures in a Pleistocene glaciolacustrine delta and their implications for the recognition of subenvironments in delta deposits, Sedimentology, 60, Pp. 637–665. doi: 10.1111/j.1365-3091.2012.01354.x

Reyment, R.A., 1965. Aspect of the Geology of Nigeria. Ibadan University Press, Pp. 145.

Selly, R.C, 2000. Applied Sedimentology (second edition). Academic press publication, Pp. 543.

Simpson, A., 1954. The Nigerian coal fields and the geology of part of Onitsha, Owerri and Benue provinces. Geological Survey Nigeria Bulletin, 24, Pp. 85.

Tijani, M.N., Nton, M.S., Kitagawa, R., 2010. Textural and geochemical characteristics of the Ajali Sandstone, Anambra Basin, SE Nigeria: Implication for its provenance. C. R. Geoscience, 342, Pp. 136–150

Uzoegbu, M.U., Ikwuagwu, C.S., 2016. Sedimentological characteristics of Ajali sandstone at Okigwe, Anambra basin, SE Nigeria. International Journal of Geology and Mining, 2, 1, Pp. 38-52.

Valente, A. Ślączka, A., Cavuoto, G., 2014. Soft-sediment deformation structures in seismically affected deep-sea Miocene turbidites (Cilento Basin, southern Italy). Geologos 20, 2, Pp. 67–78. doi: 10.2478/logos-2014-0009.

Van Asselen, S., 2011. The contribution of peat compaction to total basin subsidence: Implication for the provision of accommodation space in organic-rich deltas. Basin Research, 22, 2, Pp. 239-255. https://doi.org/10.1111/j.1365-2117.2010.00482.x

Wentworth CK. 1922. A scale of grade and class terms for clastic sediments. Journal of Geology, 30, Pp. 377–392.

Whiteman, A., 1982. Nigeria: Its Petroleum Geology, Resources and Potentials. Vol. 1 and 2. Graham and Trotman Ltd.: London. UK.